Pressure maxima in the flow of superfluid ^{4}He in tubes

Gary L. Mills, Allan J. Mord, and Howard A. Snyder
Ball Electro-Optics and Cryogenics Division, P.O. Box 1062, Boulder, Colorado 80306
and University of Colorado, Campus Box 429, Boulder, Colorado 80309
(Received 1 October 1993)

Calculations based on the standard equations for the flow He II in tubes predict large pressure and moderate temperature maxima when the tube is long and narrow. This effect has not, to our knowledge, been previously observed. Experimental data are presented that confirm the existence of the pressure maxima in capillaries of diameter 0.3 μm. The measured data are in good agreement with predictions. The data validate the model equations for flow in capillaries and porous media using the bulk value of the Gorter-Mellink parameter. This effect may impact interpretations of experimental searches for size effects.

Over the past eight years two of the present authors have developed several numerical models for the flow of He II based on the Landau equations with the Gorter-Mellink interaction.[1-3] The most recent code, called SUPERFLOW, was used to make a comprehensive study of the flow through tubes under a wide variety of conditions.[4] These calculations show an interesting and physically important effect not hitherto reported in the literature: large pressure and moderate temperature maxima along long and narrow tubes. The results of an experiment presented here to demonstrate the maxima agree very well with the model predictions.

The physical origin of the maxima is the conversion of some of the superfluid component of He II to normal fluid as the temperature rises. When the temperature and the chemical potential increases in the same direction (the usual situation) the superfluid component flows toward the warm end. As the superfluid component ρ_s flows up the thermal gradient, some is converted to normal component ρ_n to maintain the correct ratio ρ_n/ρ_s for the local temperature. This is equivalent to ρ_n flowing in through the walls of the tube and ρ_s flowing out. The additional ρ_n must flow out the ends of the tube to maintain a steady state with constant mass flow. If the length to diameter ratio L/D is large, sufficient pressure builds up to force the additional ρ_n out both ends of the tube. This effect is important in confined regions such as porous materials and long thin tubes. An accompanying temperature maximum sometimes results from thermodynamic considerations.[4]

These maxima are newly recognized phenomena of He II flow that are inherent in the accepted equations of motion. Practical applications of He II flow, such as porous plug pumps and cooling systems for superconducting magnets, require a knowledge of when and where the maxima occur and how large they are. An important research application is in the analysis of experimental measurements on the phase transition in confined spaces. Recent experiments have been carried out in aerogels where this effect becomes large; see Ref. 5 and the references cited therein. For these materials, a very small temperature difference across a sample can lead to significant pressure and temperature shifts inside the sample. Thus, a pressure measurement at the surface may not correspond to the interior pressure. The model used here predicts how large a temperature difference can be tolerated if the limits on the pressure and temperature shifts inside are to be held within specified limits. This information is needed for the design of experiments and the analysis of their results.

The mass, energy, and momentum conservation equations of the model can be written as

$$\dot{M} = A\rho_s v_c + A\rho v_n \ , \tag{1}$$

$$\frac{dE}{dx} = \dot{M}\frac{dh}{dx} + \frac{dQ_{ic}}{dx} \ , \tag{2}$$

$$a\rho_n v_c^3 = -\frac{d\mu}{dx} = s\frac{dT}{dx} - \frac{1}{\rho}\frac{dP}{dx} \ , \tag{3}$$

$$\eta F v_n = -\frac{dP}{dx} \ , \tag{4}$$

where v_s and v_n are the superfluid and normal component velocities, the relative counterflow velocity is $v_c = v_s - v_n$, $\dot{M}$ is the mass flow rate, A is the flow area, dE is the power added to an element of line dx, a is the Gorter-Mellink parameter, h, s, and μ are the specific enthalpy, entropy, and chemical potential, and η is the viscosity. F, the classical friction factor for the normal component, depends on Reynolds number. The thermodynamic pressure, $P = p + \rho g z$, takes into account the gravity head. The internal convection Q_{ic} is

$$Q_{ic} = -A\rho_s s T v_c \tag{5}$$

These commonly accepted equations for one-dimensional steady-state He II flow result from averaging the more general equations over a cross section of the flow channel. The approximations, assumptions, and limitations of this set of equations and their relation to others are discussed at length elsewhere.[4] Because the numerical model treats the flow path from end to end, it automatically satisfies the boundary conditions at the interfaces between

different flow channels. Porous materials are modeled as parallel paths. There is a provision for side wall heating in the numerical model.

Because there are four unknowns in the model, at least four physical parameters of the system must be measured simultaneously to verify the equations. We surveyed the literature in an effort to test the numerical model and found that most investigators have not reported the simultaneous measurement of four parameters. The data from the few studies with the required measurements (only three were found) showed excellent agreement with the model.[3] None of the surveyed articles reported the pressure and temperature maxima.

The purpose of this experiment is to show that the pressure and temperature maxima occur and that they are accurately predicted by the model. This is the most severe test of the model equations reported to date. Previous work has covered a range of conditions corresponding to values of the dimensionless parameter σ (Ref. 4) from -0.3 to about $+1$ (Ref. 3). This experiment extends to $\sigma=250$. Thus, a second purpose is to show that the model is valid for analyzing experimental data in extreme flow conditions.

The maxima occur near the midpoint of tubes for which L/D is large. Since it is not possible to put pressure and temperature sensors in the walls of thin capillaries where the maxima occur, we cut the tube and insert large diameter test sections with sensors. Calculations show that the p and T profiles in the capillary are nearly the same as before the cut was made. This is the basis of our experimental design.

The apparatus (Fig. 1), which is about 12 cm in diameter, is immersed in a 20-cm i.d. dewar. He II flows between the 5 liter volume A and the main dewar (volume B) through the 1×12 cm flow path. The flow path has four test sections each with a germanium thermometer and silicon pressure transducer. One temperature transducer was not operating properly so only three temperatures were obtained along the flow path. There are 17 porous alumina filter disks[6] in the flow path: four between each pair of test sections, two at the bottom, and three at the top. The heights of He II in volumes A and B are monitored with superconducting liquid level probes. The temperatures at the free surfaces are set separately by pumping. Heaters are provided in both dewars to maintain a steady temperature difference across the flow path. The temperature and pressure sensors were calibrated in place as part of the experiment each day.

These porous disks were chosen because they have a simple cylindrical channel structure and provide many parallel narrow tubes. Electron microscopy showed that the channels are nearly straight and have very few cross links. They taper, on average, from 0.229 to 0.294 μm over a length of 60 μm, with a standard deviation from sample to sample and channel to channel of about 0.021 μm. The manufacturer quoted porosity of 50% seems consistent with the electron microscope photos. Some of the channels are dead ended, so the conventionally measured porosity overestimates the number of open channels per unit area slightly.

The He II flow is controlled by the pressure and temperature differences across the flow path. Since most of the properties of He II vary rapidly with temperature, data was taken in the 2.0-K range, and at lower temperature in the 1.6-K range. We compared flows upward toward A and downward toward B. Figure 2 shows a low-temperature run with flow from B to A that is driven primarily by a temperature difference and Fig. 3 is a similar run at a higher temperature. Figure 4 shows a flow from

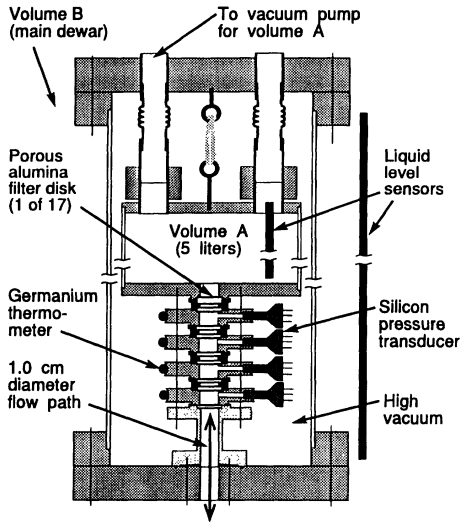

FIG. 1. Schematic of apparatus.

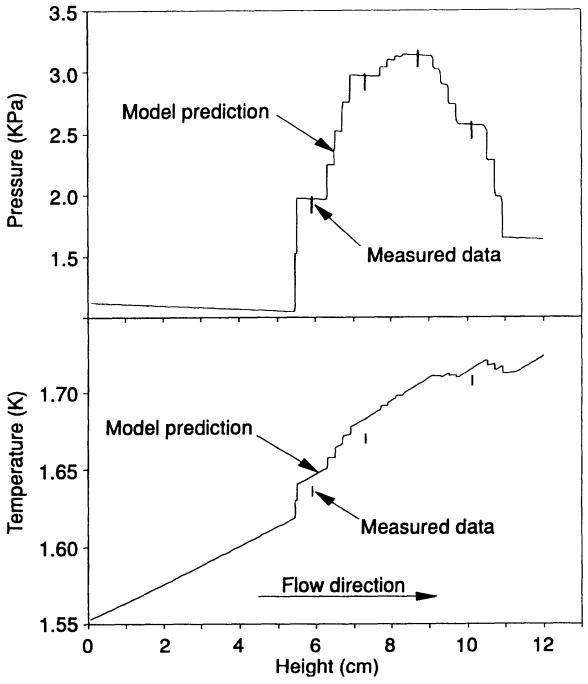

FIG. 2. Pressure and temperature profiles for a low-temperature run with the flow upward from B to A. Vertical bars give measured data $\pm$ two standard deviations; the solid line is the model prediction.

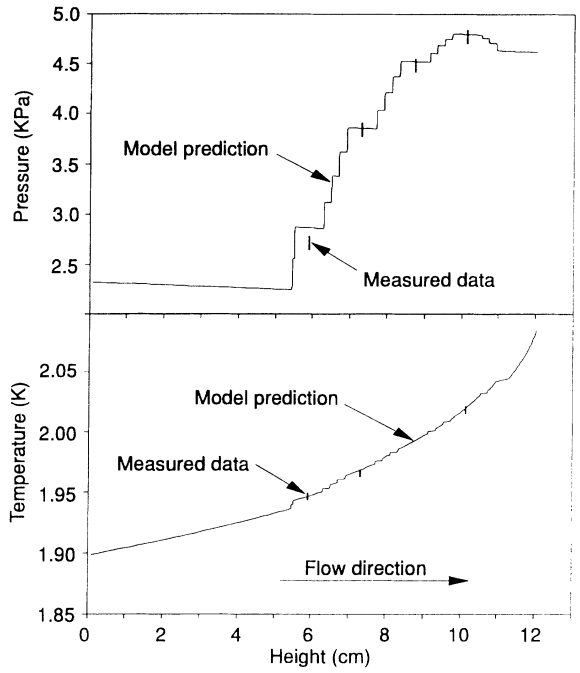

FIG. 3. Pressure and temperature profiles for a high-temperature run with flow upward from B to A.

A to B in the low-temperature range. The measured inlet and exit temperature and pressure of the flow path, corrected for gravity head, and the sensor heat input are used to predict the profiles.

The agreement between the predictions and the experimental data is very good. The total standard deviation for noise and calibration uncertainty is 35 Pa for the pressure and 1.6 mK for the temperature. Nearly all the pressure data agree with the model predictions to within two standard deviations. The temperature data is systematically lower than predicted by as much as 10 mK when the flow is from B to A, and higher by up to 5 mK when the flow is in the opposite direction. On the scale of the total 200 mK temperature difference, this is a small effect; but it is much larger than the known uncertainties. It occurs in all runs and is systematic in that all sensors show a proportionate deviation. Including the gravitational pressure head term in the energy Eq. (2) will not account for the discrepancy. It is not a calibration error since the deviation changes sign with flow directions. At present it is unexplained.

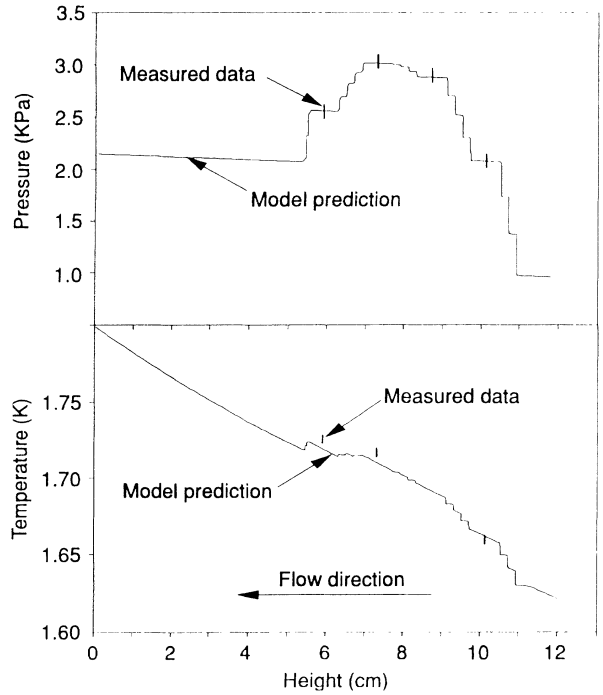

FIG. 4. Pressure and temperature profiles for a low-temperature run with flow downward from A to B.

The mass flow is determined from the height data. The heat flux is estimated from the known heat leaks and the heater power needed to produce steady-state conditions. Both the mass flow and internal heat convection data agree with the predictions to within experimental uncertainties.

This experiment demonstrates the existence of the pressure peaks and validates the model even under extreme conditions. Agreement this good is somewhat unexpected. No adjustable parameters are used. We have measured the pore size and used the manufacturer's value of the porosity. All the thermodynamic properties and the transport coefficients are taken from the literature; (see Ref. 3 for the source of the data and a discussion of its uncertainty). All the thermodynamic data and transport coefficients that appear in Eqs. (1)–(4) are known to better than 3% except the Gorter-Mellink parameter a, which has a spread among measured data of $\pm 40\%$.[7,8] We have used Schwarz's calculated values[8] of a. Another error source is the large variation in channel size in the porous disks. We have modeled straight, uniform, 0.27-μm channels, which is the average size at the midpoint of the tube. We have neglected the tapering of the channel as well as any entrance or exit effects between the porous disks and the test sections. The uncertainty of a and the spread of the pore diameters are therefore the two major sources of error in our calculations.

We have explored the sensitivity of the model output to changes in porosity, pore size, and the a parameter for the conditions corresponding to Fig. 2. Table I shows the changes in several output variables for 1% increase of the input. Here, p_3 and T_3 refer to the third test section and are normalized by the total pressure or temperature difference across the flow path.

It is clear that pressure is the most sensitive of these

TABLE I. Change in output variables for a 1% increase in parameters for conditions corresponding to Fig. 2.

Input parameters	Mass flow	Internal convection	p_3	I_3
Porosity	+1.0%	+1.0%	−1.6%	−0.1%
Pore size	+.04%	+.04%	−6.0%	−0.3%
a	−0.3%	−0.3%	−1.3%	−0.8%

variables to changes in the input parameters surveyed. The excellent agreement of the pressure profiles would be lost if any of these parameters were changed by more than ±5%. The data, therefore, show that the Gorter-Mellink term, as it appears in Eq. (4), and a from Ref. 8 are adequate to predict flows in channels as small as 0.3 μm. We find no evidence for the dependence of Eq. (4) and/or the a parameter on pore size in our data.

The results show the importance of maintaining isothermal conditions throughout samples when size effects are measured. The pressure and temperature shifts increase nonlinearly as the temperature difference and the length of the sample increase or as the pore size decreases.[4] Because of the wide diversity of experimental apparatus used in these studies, each situation requires a separate analysis. We have analyzed three early studies of the depression of the λ point that report sufficient details on the experimental equipment[9] and found that for some measurements up to half the inferred depression can be attributed to thermal gradients in the sample.

This work was supported by Ball Electro-Optics and Cryogenics Division and by the Superconducting Super Collider Laboratory through Contract No. 92-Z09578.

[1]L. A. Hermanson, A. J. Mord, and H. A. Snyder, Cryogenics **26**, 107 (1986).

[2]H. A. Snyder, Cryogenics **28**, 86 (1988).

[3]A. J. Mord, H. A. Snyder, and D. A. Newell, Cryogenics **32**, 291 (1992).

[4]H. A. Snyder and A. J. Mord, J. Low Temp. Phys. **86**, 177 (1992).

[5]M. Larson, N. Mulders, and G. Ahlers, Phys. Rev. Lett. **68**, 3896 (1992).

[6]Anodisc (trademark) model 20013. Anotec Separations Ltd., Widmere Road, Barbury, Oxon, England.

[7]J. T. Tough, in *Progress in Low Temperature Physics,* edited by D. F. Brewer (North-Holland, Amsterdam, 1982), Vol. VIII, p. 133.

[8]K. W. Schwarz, Phys. Rev. B **18**, 245 (1978).

[9]H. A. Snyder and A. J. Mord, Bull. Am. Phys. Soc. **37**, 1758 (1992).

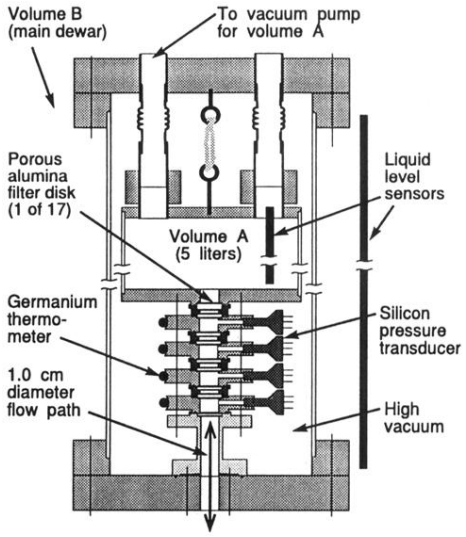

FIG. 1. Schematic of apparatus.